

Real Time Tire Soil Parameters of a Tractor in Tillage Applications

Jan Wieckhorst, Thomas Fedde, Ludger Frerichs

The losses occurring in the tire-soil contact dominate the system efficiency of a tractor in tillage applications. The operator can minimize these losses by adjusting the ballasting and the tire inflation pressures of the tractor. Analyzing scientific publications on off-highway traction shows that the lowest permissible tire inflation pressure does not necessarily lead to maximal tractive efficiency. The tire inflation pressure for maximal tractive efficiency has to be determined for the current traction conditions. Therefore, tire-soil mappings for different tire inflation pressures were generated from sensor data and evaluated based upon the resulting tractive efficiencies. The investigations initially confirm that working at the edge of the tire load capacity does not always lead to maximum tractive efficiency. The evaluation of different tire pressures on the basis of tire-soil mappings is suitable for homogeneous traction conditions, while the evaluation of heterogeneous traction conditions needs further research.

Keywords

Tractors, traction, central tire inflation system, tire-soil mappings, optimization, sensors

During the course of agricultural engineering history, the tractor developed from a replacement for horses pulling implements to a multifunctional mobile working machine. Today the tractor is the key machine in industrial agriculture. This has been made possible due to the standardization of interfaces to attach implements to the tractor and to transfer power from the tractor to the implement. Heavy traction applications on agricultural soils are still a big part of the duty cycle of a tractor. The relevance of the tractive efficiency is linked to the economic impact of the fuel consumption in arable farming and the related CO₂-emissions (FRERICHS et al. 2017). Figure 1 shows an exemplary power flow diagram of a tractor performing a heavy tillage application.

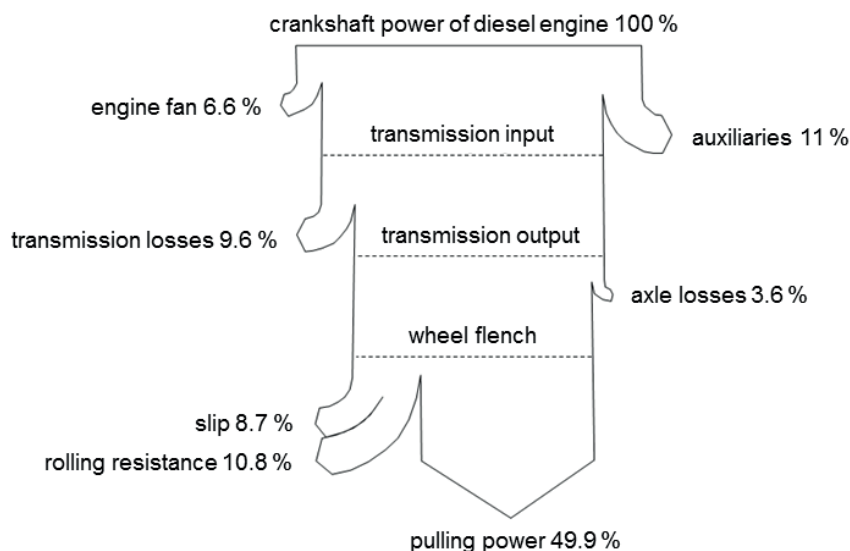


Figure 1: Power flow diagram of a tractor during a heavy tillage application (PICHLMAIER 2012)

The biggest losses when converting the crankshaft power of the diesel engine into tractive power at the drawbar occur in tire-soil-contact caused by slip and rolling resistance. These losses can be minimized by ballasting and adjusting the tire inflation pressure of the tractor. When adjusting the tire inflation pressure it has to be noted that the tire load capacity (i.e. the maximum permissible vertical wheel force) depends on the tire inflation pressure. In this context, the tire utilization factor is often used. The tire utilization corresponds to the quotient of the current vertical wheel force and the maximum permissible vertical wheel force at the current working speed and the current tire inflation pressure. A tire utilization of 100% means that the tire is operated at the limit of its tire load capacity. According to common best practice, the lowest possible tire inflation pressure is considered the most efficient for pulling applications on agricultural soils. Investigations by STEINKAMPF (1986), REMPFER (2003) and WETTEMANN (2012) show that working at the edge of the tire load capacity is not always optimal in terms of efficiency.

STEINKAMPF (1986) published more than 700 tire-soil mappings, which were measured with a test rig on agricultural soils at the Research Institute for Agriculture (FAL) in Braunschweig. When plotting the traction parameters over the slip, the tractive efficiency initially increases steeply above the slip and decreases almost linearly after reaching the maximum efficiency (Figure 2). Figure 2a shows the tractive efficiency curve achieved with bias-ply tires on clay with untreated stubble. The tire inflation pressure has been set to 1.4 and 1.1 bar. The higher tire inflation pressure of 1.4 bar results in a higher tractive efficiency in the entire mapping. However, for the mappings produced on a ploughed, loamy sand with the same tires, the lower tire inflation pressure of 1.1 bar leads to higher tractive efficiencies (Figure 2b). The rolling resistance, also measured by STEINKAMPF, increases when the tire inflation pressure is reduced. This has a negative impact on the tractive efficiency. The stiffness of the carcass of bias-ply tires is higher than the stiffness of the carcass of radial tires. The tires flex significantly more with reduced tire pressure, which leads to a bigger increase of the internal rolling resistance for the bias-ply tires than for the radial tires with relatively soft sidewalls.

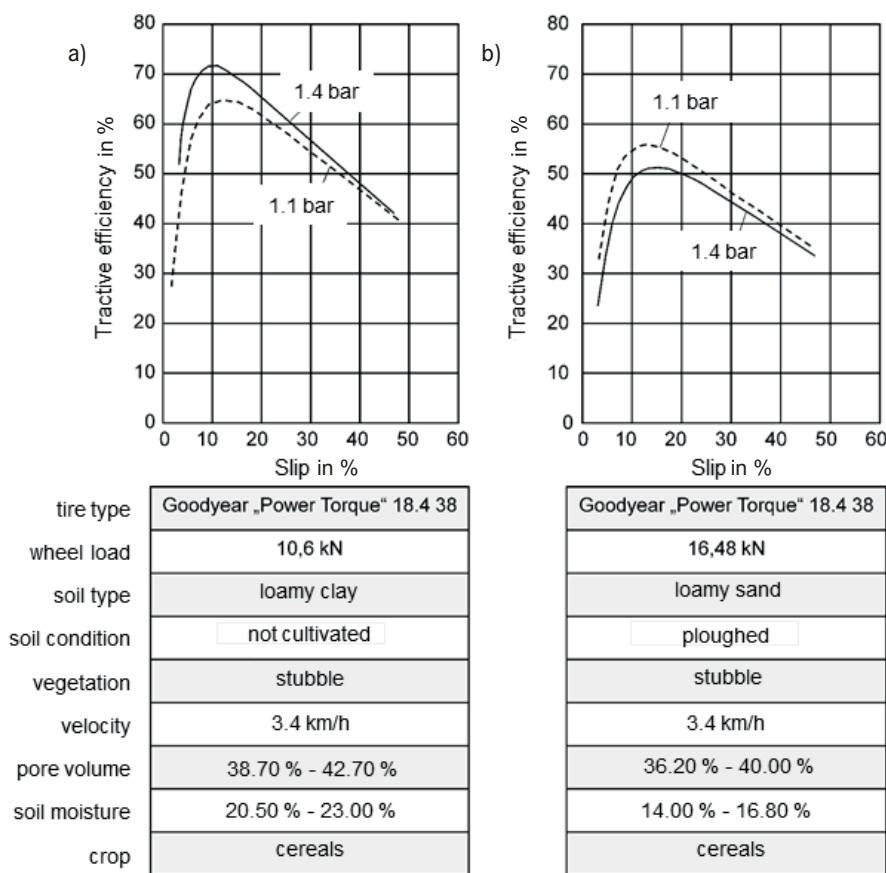


Figure 2: Tire-soil mappings - tractive efficiency plotted over slip for different traction conditions and tire inflation pressures (STEINKAMPF 1986)

REMPFER (2003) discusses the basics of central tire inflation systems for tractors. He answers both conceptual questions on the system and the influence of tire inflation pressure on the duty cycle of the tractor drivetrain and structure. Furthermore, he investigates the impact of the tire inflation pressure on different traction parameters. REMPFER measured these traction parameters by using a test tractor, which has been equipped with several sensors. Figure 3 shows the traction force and the rolling resistance coefficients as well as the slip values and tractive efficiencies measured during sub-soiling with standard tires on a clayey luvisol with different tire inflation pressures. The maximum tractive efficiency is obtained at a tire inflation pressure of 0.8 bar and not with full tire utilization at a tire inflation pressure of 0.6 bar. The reason for this is the rolling resistance coefficient, which increases when the tire inflation pressure is reduced from 0.8 to 0.6 bar, whilst the traction coefficient and the slip stay almost constant.

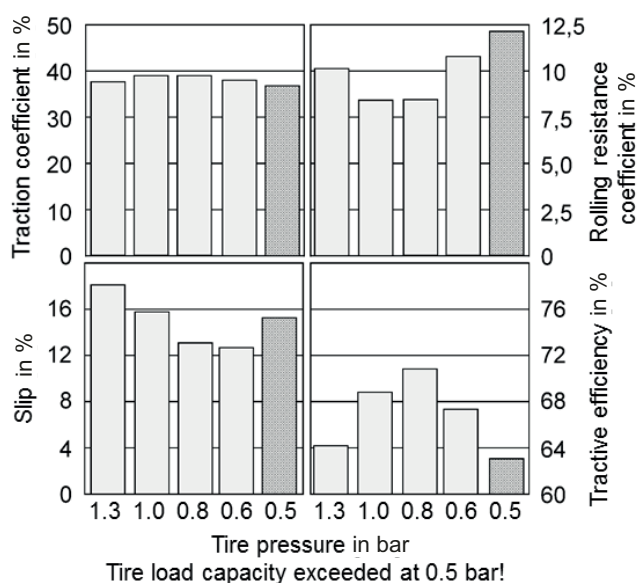


Figure 3: Traction parameters of a tractor whilst subsoiling with different tire inflation pressures (REMPFER 2003)

WETTEMANN (2012) compared the fuel consumption and the slippage of a tractor during pulling applications on dry, loamy sand. The measurements were carried out with and without ballasting of the tractor and at tire inflation pressures of 1.6 bar, 0.8 bar and 0.6 bar. Minimum fuel consumption and slippage resulted from the measurement with a tire inflation pressure of 0.8 bar (Figure 4). WETTEMANN explained this with a reduced surface pressure within the tire soil contact due to the increased contact surface. The reduced surface pressure has a negative impact on the grip of the tire and leads to an increase in slip at the minimal tire inflation pressure for the given traction conditions.

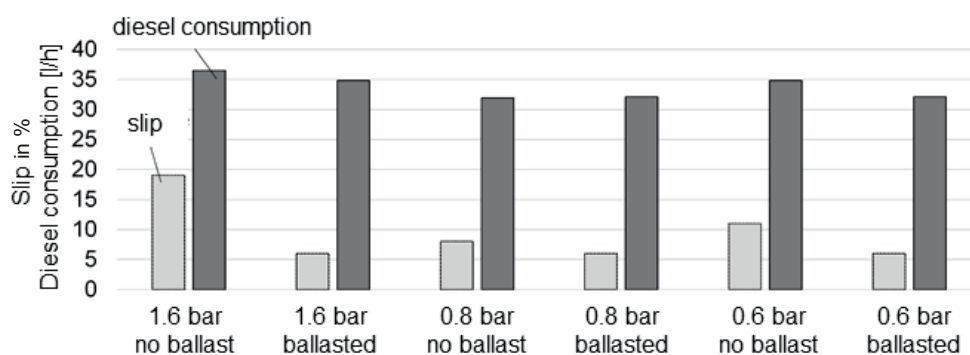


Figure 4: Slip and diesel consumption during pulling work on loamy sand at different tire inflation pressures (WETTEMANN 2012)

Method for Optimizing the Tractive Efficiency by Adjusting the Tire Inflation Pressure

The tire inflation pressure, which leads to the highest tractive efficiency, depends on the actual operating conditions. To optimize the tractive efficiency by adjusting the tire inflation pressure, it is not sufficient to just compare the tractive efficiencies measured at different tire inflation pressures. When comparing different tire inflation pressures in regards to the achievable tractive efficiencies,

the location of the operating point in the tire-soil mapping must be taken into account. In Figure 5, the tractive efficiency is not plotted over the slip, like in Figure 2, but over the traction coefficient. In this type of diagram, the tractive efficiency initially rises steeply above the traction coefficient and then, after reaching a bulky area of maximum efficiency, it drops steeply at higher traction coefficients.

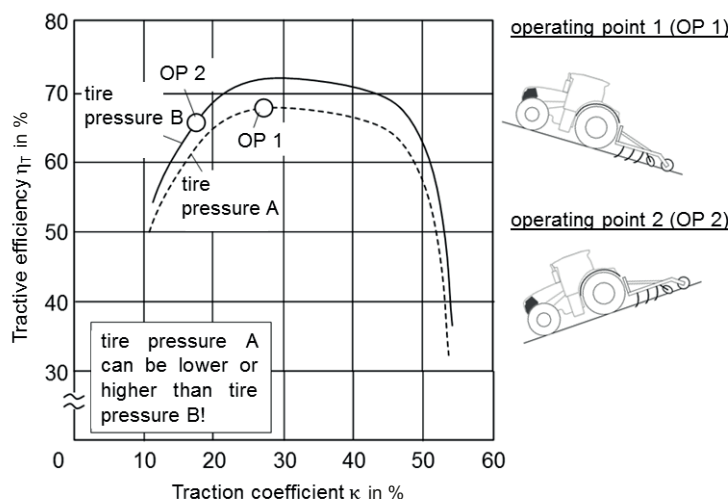


Figure 5: Comparison of two operating points in the tire-soil mapping concerning the achievable tractive efficiencies at different tire inflation pressures according to WIECKHORST et al. (2017)

The tractive efficiency η_T is calculated as the quotient of the output and the input power of the traction drive (Equation 1):

$$\text{Tractive efficiency: } \eta_T = \frac{P_{out}}{P_{in}} = \frac{v \cdot F_T}{\omega \cdot T} \tag{Eq. 1}$$

For a wheel, the output power is the product of the working speed v and the traction force of the wheel F_T , while the input power corresponds to the product of the wheel angular speed ω and the wheel torque T .

The traction coefficient κ corresponds to the ratio of the horizontal force F_T and the vertical force F_G at the traction drive (Equation 2):

$$\text{Traction coefficient: } \kappa = \frac{F_T}{F_G} \tag{Eq. 2}$$

The wheel traction force F_T is the horizontal wheel force and the wheel load F_G is the vertical wheel force. Operating point 1 in Figure 5 is located on the characteristic curve of the tractive efficiency for tire inflation pressure A within the point of maximum tractive efficiency at a traction coefficient of 27%. Operating point 2 is located on the characteristic curve of the tractive efficiency for tire inflation pressure B further left in the mapping with a traction coefficient of 17%. Although the efficiency curve for tire inflation pressure B is higher than the one for tire inflation pressure A in the entire mapping, a simple comparison of the tractive efficiencies achieved in the two operating points

leads to the erroneous assessment that higher tractive efficiencies can be achieved with tire inflation pressure A. In practice, the different locations of the operating points on the characteristic curve for the respective tire inflation pressure can also be caused at constant working depth and speed. For example, if the tractor is working uphill in operating point 1 it has to overcome the gradient resistance in addition to the draft force of the implement. When the tractor is working downhill in operating point 2, the inertia forces of tractor and implement act in the direction of travel of the tractor.

When comparing different tire inflation pressures regarding the tractive efficiencies, the tire-soil mappings must be generated from sensor data. To do so, the tractive efficiency is classified over the traction coefficient. Figure 6 shows an example of the evaluation of two tire-soil mappings RK and RK^* , each generated at different tire inflation pressures. The comparison of the tractive efficiencies achieved with the different tire inflation pressures is only permissible in the area of the overlapping of the tire-soil mappings. To evaluate the tire inflation pressures, the values of all classes of both maps RK and RK^* in the range between the higher of the lower traction coefficients κ_{min} and the lower of

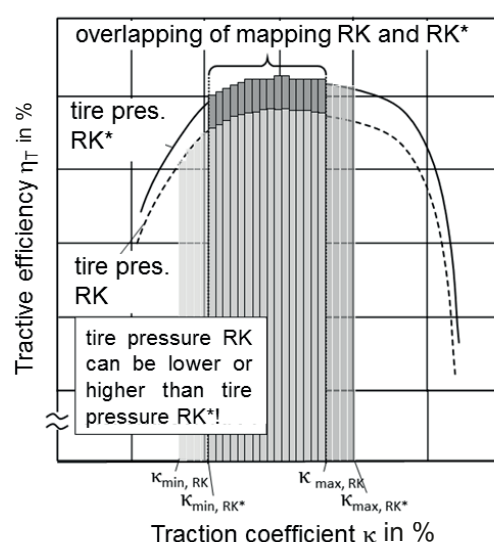


Figure 6: Evaluation of the classified tire-soil mappings generated from sensor data according to WIECKHORST et al. (2017)

the higher traction coefficients κ_{max} are added up.

Subsequently, the sum of all classes of the lower tire inflation pressure in the overlap area is subtracted from the sum of all classes in the overlap area of the higher tire inflation pressure (Equation 3):

$$\sum_{\kappa_{min,RK^*}}^{\kappa_{max,RK}} \eta_{T,RK^*}(\kappa) - \sum_{\kappa_{min,RK^*}}^{\kappa_{max,RK}} \eta_{T,RK}(\kappa) \tag{Eq. 3}$$

If the result is positive, this means that higher tractive efficiencies are achieved with tire inflation pressure RK^* than with tire inflation pressure RK . If the result is negative, the tire inflation pressure RK leads to higher tractive efficiencies.

When evaluating different tire inflation pressures by generating tire-soil mappings, it should be noted that these mappings are always generated under constant (i.e. homogeneous) traction conditions. If sensor data collected under heterogeneous traction conditions is written into the same tire-soil mapping, an arithmetically averaged tire-soil mapping is generated. This does not represent the traction behavior of the tire used at a certain tire inflation pressure on a certain soil with a certain soil condition, but a theoretical traction behavior by averaging the traction parameters measured on different soils and soil conditions. In this study, the data was collected under homogeneous traction conditions, when generating characteristic mappings with the test tractor.

Traction Sensors within the Test Tractor

Figure 7 shows the sensors used to generate the mappings for one of the rear wheels of the test tractor. The working speed is determined with a GPS sensor attached to the cab of the tractor. The angular speed of the rear wheel is calculated from the output speed of the gearbox, taking into account the ratios of the drive train. Due to the balancing function of the rear axle differential, it must be ensured that the differential lock is activated during the measurements with the test tractor. Alternatively, it has to be driven in a straight line with the same traction conditions between the wheels of the axles. A new type of sensor for traction parameters measures the vertical and horizontal wheel forces as well as the wheel torque. This traction sensor is based on the principle of the inverse magnetostriction and was presented in detail in WIECKHORST et al. (2015) and PEETERS et al. (2017). The sensor is not installed on the left side of the rear axle as displayed in Figure 7, but on the right side. As a reference for the horizontal wheel force (wheel traction force) measured by the traction sensor, the test tractor was also equipped with a ball-type hitch, which measures the interface forces with resistance strain gauges.

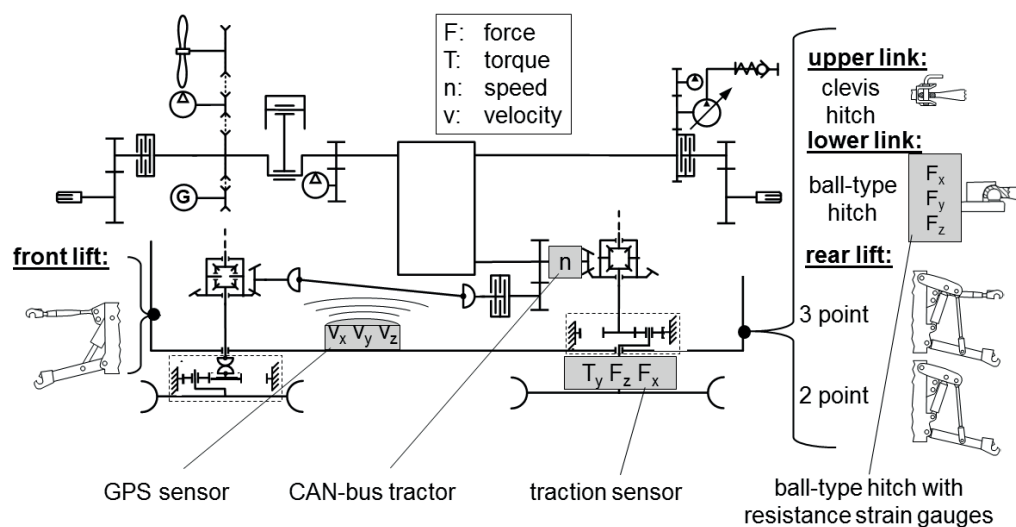


Figure 7: Sensors in the drive train of the test tractor according to (WIECKHORST et al. 2015)

Commissioning of the Sensors in the Test Tractor

After installing the sensors in the test tractor, some tests were carried out on tarmac. This ensured the transferability of the results from the test bench tests to the sensors installed in the tractor and the plausibility of all traction parameters calculated from the sensor signals. Figure 8 shows the signals for the horizontal and the vertical wheel force over time when lifting a rear weight. In addition, the readings from the rear wheel weighing plate for the lowered and lifted rear weight are shown in the diagram. After approx. 10 seconds, the rear weight was lifted and after approx. 40 seconds, it was lowered again. The maximum deviation of the values of the weighing plate and the signal for the vertical wheel force of the sensor within the rear axle of the tractor is 0.5 kN in the lowered position and 0.4 kN in the raised position. The signal noise throughout the course of the vertical wheel force in the range between 20 and 30 s is caused by getting off and on the tractor in order to read the weighing plate display values. The signal of the horizontal wheel force shows that the vertical wheel force does not have any significant influence on the sensor signal for the horizontal wheel force. The influence on the horizontal force signal of the sensor is less than 0.2 kN.

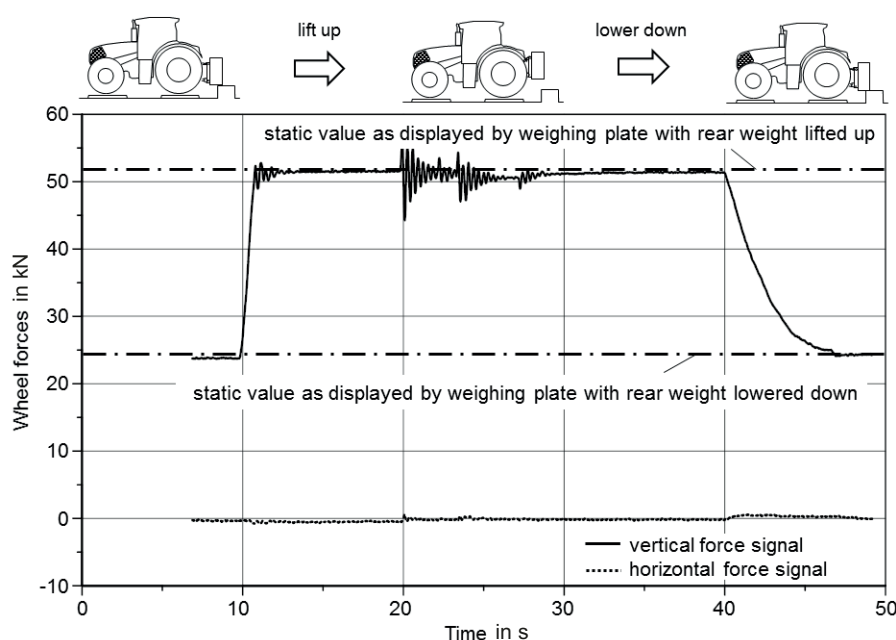


Figure 8: Analysis of the traction sensor signal for the vertical and the horizontal wheel force when lifting and lowering a rear weight on weighing plates (WIECKHORST et al. 2017)

Figure 9 shows the signals for the horizontal wheel force of the traction sensors and the halved traction force signal of the strain gauges on the ball-type hitch, when pulling a braking trailer on tarmac over time in the upper diagram. In the middle diagram, the deviation of the signal of the traction sensor and the strain gauges on the ball-type hitch is plotted over time and in the lower diagram the driving speed is plotted over time.

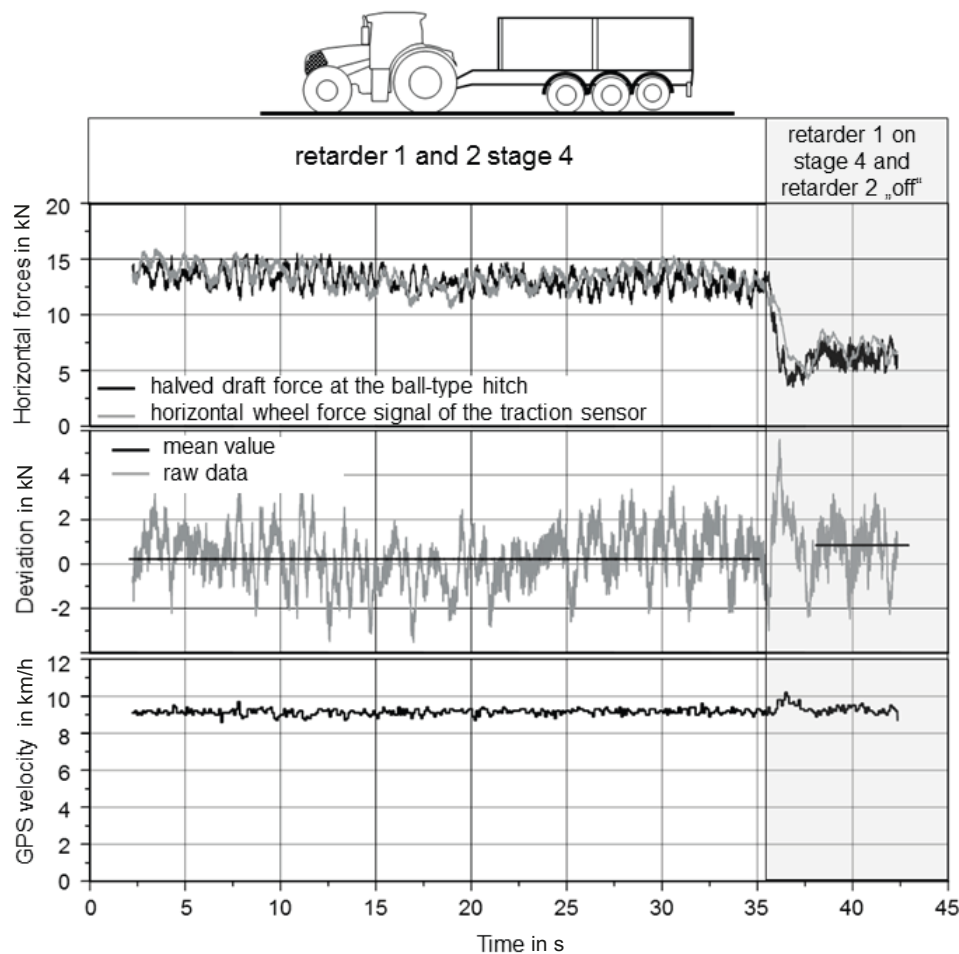


Figure 9: Comparison of the horizontal force signal of the traction sensor with the draft force signal of the strain gauges on the ball-type hitch (WIECKHORST et al. 2017)

The brake trailer is equipped with two retarder axles. With these, the braking force can be adjusted in four stages. The four-wheel drive of the tractor was not active during the entire measurement, whilst the tire inflation pressure on both axles of the tractor was set to 1.6 bar and the driving speed was 9 km/h (cruise control). At the beginning of the measurement, both retarder axles were activated at level 4. After about 35 s, one of the retarder axles was switched off. The signal for the horizontal wheel force follows the signal for the halved draft force measured at the ball-type hitch well. As the all-wheel drive was not active, the rear wheels of the tractor had to overcome the rolling resistance of the front axle in addition to the draft force of the brake trailer. The expected difference between the traction force of the rear wheel and half of the total draft force at the ball type hitch is 0.19 to 0.38 kN. The rolling resistance coefficient on tarmac is between 1.5 and 3% (STEINKAMPF 1986). For the calculation of the front axle load, the position of the center of gravity and the geometry parameters of the tractor as well as the forces acting on the ball-type hitch have been taken into account. In the first part of the test run with both retarder axles fully activated, the traction force of the wheel measured by the sensor installed within the rear axle of the tractor is in average 0.21 kN higher than the halved tractive force measured with the resistance strain gauges at the ball-type hitch, and thus within the expected range. After switching off one of the retarder axles, the resulting deviation of 0.7 kN is

higher than the maximum expected value of 0.38 kN. The reason for this is the decreasing measuring accuracy of the force signals of the traction sensor in the range between the wheel traction forces used for the two-point calibration of the signals on a test bench.

Results from the Measurements with the Test Tractor

The first test runs with the test tractor to generate tire soil mappings at different tire inflation pressures were carried out on tarmac. With this, all influences on the sensor signals from the heterogeneity of the soil and its influence on the traction behavior were avoided. The draft force was applied with the brake trailer at a constant driving speed of 12 km/h (cruise control). The all-wheel drive of the tractor was not active during the measurements carried out on tarmac. Both retarder axles of the brake trailer were activated at stage 4, which is the highest setting. In the first measurement, the tire inflation pressure on all four wheels of the tractor was 1.6 bar, while in the second measurement the tire inflation pressure has been reduced to 0.6 bar.

Figure 10 shows the tire-soil mappings generated from the measurement data. In the left diagram, the data points of the tractive efficiency are plotted over the traction coefficient. In the diagram on the right, the mean values of the tractive efficiency have been classified over the traction coefficient. With a tire inflation pressure of 1.6 bar, average tractive efficiencies between 85 and 90% are achieved. A tire inflation pressure of 0.6 bar leads to tractive efficiencies between 74 and 76%. In both cases the traction coefficients vary between 30 and 35%. The big difference between the tractive efficiencies achieved with the two different tire inflation pressures of well over 10% in the entire mapping is plausible. With the lower tire inflation pressure the tires were flexing a lot, which resulted in an increase of the internal rolling resistance of the tires.

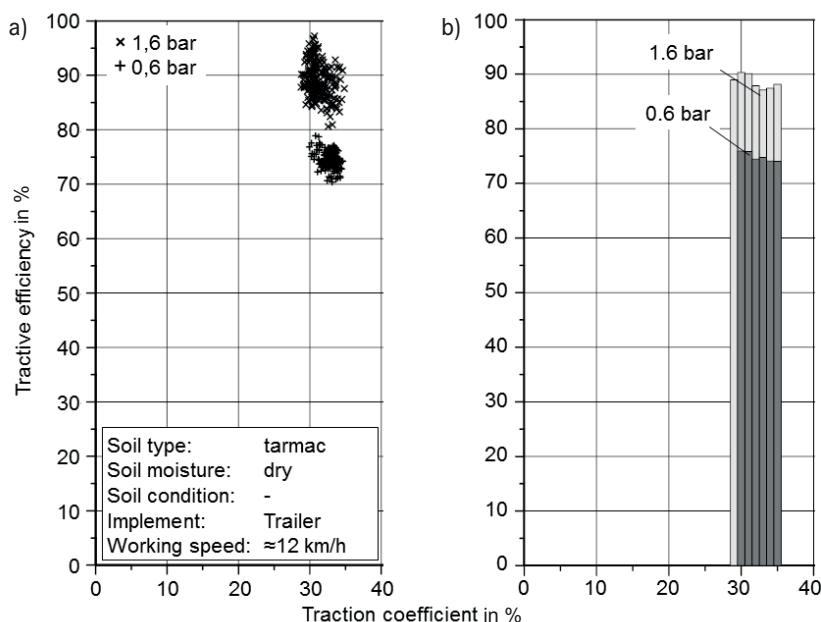


Figure 10: Tire-soil mappings for pulling work on tarmac at 12 km/h with different tire inflation pressures – a) data points and b) classified data according to (WIECKHORST et al. 2017)

Figure 11 shows the classified tire-soil mappings generated from measurement data of the test tractor collected during shallow soil cultivation with a mounted chisel plow on dry, loamy sand. The tire inflation pressure was set to 0.7, 0.8, 0.9 and 1.0 bar and the tire load capacity was not exceeded in any of the measurements. As before, the tractive efficiency was plotted over the traction coefficient. All-wheel drive was activated for all four measurements. The working speed was 10 km/h and the engine load was 100%. After each adjustment of the tire inflation pressure, the working depth was checked and adjusted by changing the length of the top link (rear lift in floating position).

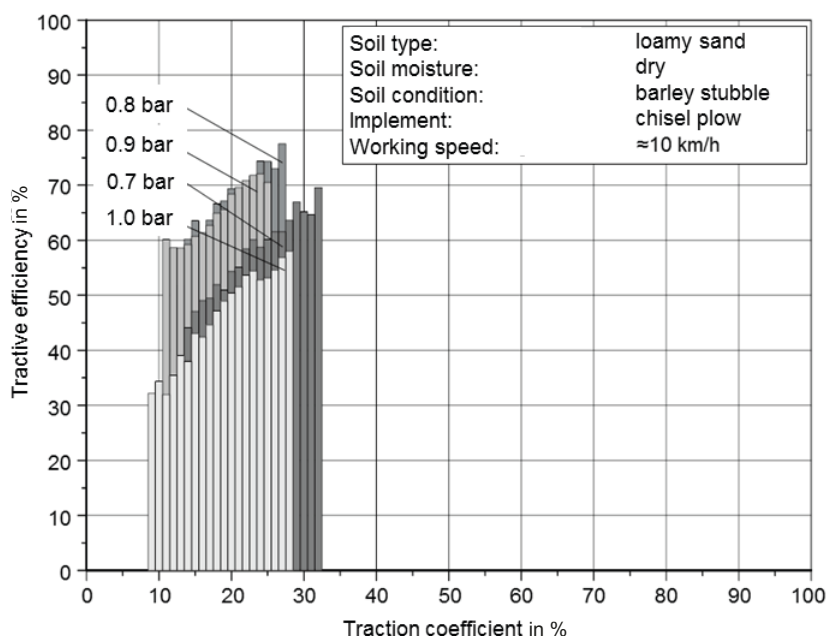


Figure 11: Tire-soil mappings of the measurements with different tire inflation pressures whilst shallow cultivation on barley stubble and dry, loamy sand (WIECKHORST et al. 2017)

When looking at the tire-soil mappings, it is initially noticeable that the traction coefficient was between 10 and 30% for all test runs. In this range, the course of the tractive efficiency increases above the driving force coefficient (Figure 5). The maximum efficiency of the curves at higher traction coefficients was not reached during any of the measurements. Tractor, ballasting and implement were not optimally matched. Maximum tractive efficiencies resulted from tire inflation pressures of 0.8 and 0.9 bar. The tractive efficiency during the test run with 0.7 bar tire inflation pressure was more than 10% below the tractive efficiencies achieved at 0.8 and 0.9 bar in the entire tire-soil mapping. The lowest tractive efficiencies were achieved during the measurement with a tire inflation pressure of 1.0 bar (Equation 4):

$$\sum_{\kappa = 14 \%}^{\kappa = 25 \%} \eta_{T,0,8 \text{ bar}}(\kappa) > \sum_{\kappa = 14 \%}^{\kappa = 25 \%} \eta_{T,0,9 \text{ bar}}(\kappa) > \sum_{\kappa = 14 \%}^{\kappa = 25 \%} \eta_{T,0,7 \text{ bar}}(\kappa) > \sum_{\kappa = 14 \%}^{\kappa = 25 \%} \eta_{T,1,0 \text{ bar}}(\kappa) \quad (\text{Eq. 4})$$

The results of the test runs with the chisel plow on dry, loamy sand confirm the observation known from other scientific publications that minimum permissible tire inflation pressure does not necessari-

ly lead to maximum tractive efficiencies. Under the given conditions, a tire inflation pressure of 0.8 bar was optimal. The large difference between the achieved tractive efficiencies at tire inflation pressures of 0.7 and 0.8 bar of more than 10% is surprising. For this reason, the traction sensor signals are going to be validated with measuring rims under field conditions in the next step. The tractive efficiencies of different tire inflation pressures can be compared based on tire-soil mappings generated from sensor signals.

Conclusions

The system efficiency of a tractor in tillage applications is dominated by the slip and the rolling resistance losses occurring in tire-soil contact. By adjusting the tire inflation pressure, these losses can be minimized and the tractive efficiency can be optimized. An analysis of scientific publications shows that, contrary to a common best practice, the minimum permissible tire inflation pressure does not always lead to maximum tractive efficiency. Which tire inflation pressure leads to maximum tractive efficiency depends on the given traction conditions. In order to optimize the tractive efficiency by adjusting the tire inflation pressure, tire-soil mappings have to be generated from sensor data for the current traction conditions. The classified tire-soil mappings generated from the sensor data enable the comparison of different tire inflation pressures with regard to the tractive efficiencies achievable with these under homogeneous traction conditions. In a next step the quality and accuracy of the traction sensor signals is going to be validated with measuring rims under field conditions. In addition, the optimization of the tractive efficiency with the tire inflation pressure under heterogeneous traction conditions must be developed and investigated based on the present work.

References

- Frerichs, L.; Hanke, S.; Steinhaus, S.; Trösken, L. (2017): EKoTech – A holistic approach to reduce CO₂ emissions of agricultural machinery in process chains. In: 9th AVL International Commercial Powertrain Conference, 10.–11. Mai 2017, S. 85-89
- Peeters, M.; Fedde, T.; Frerichs, L. (2017): Integrated Wheel Load Measurement for Tractors. In: VDI-Berichte Nr. 2300, 10.–11. November 2015, S. 423-430
- Pichlmaier, B. (2012): Traktionsmanagement für Traktoren. Dissertation, Technische Universität München
- Rempfer, M. (2003): Grundlagen der automatischen Reifendruckverstellung bei Traktoren. Dissertation, Technische Universität München
- Steinkampf, H. (1986): Betriebseigenschaften von Ackerschlepperreifen bei unterschiedlichen Einsatzbedingungen. Landbauforschung Völkenrode (80), S. 354 und 401
- Wettemann, P. (2012): Ackern mit weniger Diesel. Neue Landwirtschaft 4, S. 67-70
- Wieckhorst, J.; Fedde, T.; Frerichs, L.; Fiedler, G. (2015): A Tractive Sensor - Integrated Measurement of Tire Soil Parameters for Tractors. In: VDI-Berichte Nr. 2251, 10.–11. November 2015, Düsseldorf, VDI-Verlag, S. 219-226
- Wieckhorst, J.; Fedde, T.; Frerichs, L. (2017): A Traction Field Test - Real Time Tire Soil Parameters of a Tractor in Tillage Applications. In: VDI-Berichte Nr. 2300, 10.–11. November 2015, S. 431-438

Authors

Dipl.-Ing. Jan Wieckhorst is project manager for electronic tractor optimization systems at CLAAS Tractor in Paderborn, Halberstädter Straße 15–19, 33106 Paderborn, und external doctoral candidate at the Institute of Mobile Machines and Commercial Vehicles at the Technische Universität Braunschweig, Langer Kamp 19a, 38106 Braunschweig, email: jan.wieckhorst@claas.com.

Dr.-Ing. Thomas Fedde is head of the Advanced Engineering Department at CLAAS Tractor in Paderborn, Halberstädter Straße 15–19, 33106 Paderborn.

Prof. Dr. Ludger Frerichs is Director of the Institute of Mobile Machines and Commercial Vehicles and University Professor at the Technische Universität Braunschweig, Langer Kamp 19a, 38106 Braunschweig.

Note

The topic has been presented on 75th Conference LAND.TECHNIK – AgEng 2017, Hannover, 10–11 November 2017 and an abridged version was published in VDI Report No. 2300.